ACS APPLIED MATERIALS & INTERFACES

Research Article

www.acsami.org

Thorough Characterization of Sputtered CuO Thin Films Used as Conversion Material Electrodes for Lithium Batteries

Brigitte Pecquenard,*[,†] Frédéric Le Cras,*[,‡] Delphine Poinot,[†,‡] Olivier Sicardy,[‡] and Jean-Pierre Manaud[†]

[†]CNRS, Univ. Bordeaux, ICMCB, UPR9048, F-33600 Pessac, France

[‡]CEA LITEN, 17 rue des Martyrs, 38054 Grenoble, France

Supporting Information

ABSTRACT: CuO thin films were prepared by radio frequency magnetron sputtering using a copper target in a (Ar + O_2) reactive mixture. Different sputtering parameters were varied including oxygen flow rate, total pressure, target-substrate distance, substrate temperature and target orientation. As expected, the thin film chemical composition is strongly dependent on the oxygen flow rate. CuO thin films having a good electronic conductivity (9.3×10^{-1} S·cm^{-1}) were obtained with an oxygen concentration of 12%. The texture and the columnar growth are amplified when the target is tilted. Preliminary electrochemical results highlight that CuO thin film performances in lithium systems are tightly related to their morphology and structure.

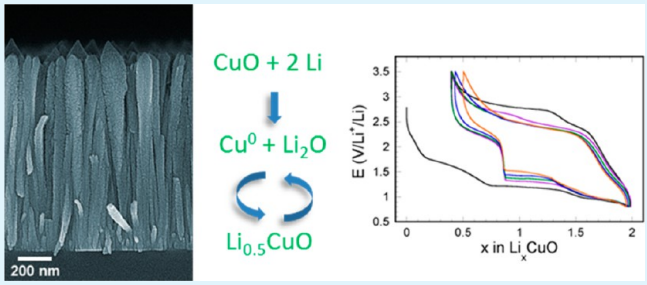

KEYWORDS: *Sputtering, CuO, thin films, lithium batteries, conversion reaction*

1. INTRODUCTION

CuO is often considered as a p-type semiconductor and, due to its properties, is useful for many applications such as transistors,[1] light emitting diodes[2] or for solar cells and electrochromic devices.[3−5] Besides, CuO is of interest in heterogeneous catalysis,[6] chemical sensors[7] and was used as an electrode material in lithium primary systems from the 1960s.[8] Li/CuO primary cells offered many advantages such as a large volumetric and gravimetric capacity, a working voltage of 1.5 V, a low discharge rate, a very low self-discharge and the possibility to be used up to 150 °C.[8] Up to two lithium ions can be electrochemically inserted into CuO according to the overall reaction, which involves the following conversion mechanism:

$$CuO + 2\,Li \rightarrow Cu^0 + Li_2O$$

During the lithium insertion, CuO is fully reduced and transforms into copper nanoparticles embedded in a Li_2O matrix. This reaction provides a theoretical capacity of 675 mAh·g^{-1} that far exceeds the specific capacity of intercalation compounds commonly used in conventional lithium-ion batteries such as $LiCoO_2$ (140 mAh·g^{-1}) or $LiFePO_4$ (170 mAh·g^{-1}).[9] As a result, the electrode material undergoes a strong morphological change upon the lithium insertion process and a volumetric expansion of 80% is expected for a CuO electrode.

More recently, CuO has attracted much attention as a negative electrode material in Li-ion batteries since Tarascon and co-workers reported the reversibility of this conversion reaction in numerous transition metal oxides.[10,11] Although CuO micrometer sized particles suffer from a poor reversibility of the conversion reaction, the latter is often greatly improved with nanostructured materials.[12−17] Only a few studies were achieved on CuO thin films, revealing that the reversibility of the reaction is even improved with thin films, making this material attractive as an electrode for Li/CuO batteries.[18−21] CuO thin films can be prepared by various techniques such as thermal oxidation of copper substrates, spray pyrolysis, electrodeposition, chemical vapor deposition or sputtering.[18−25] Until now, very few studies were devoted to the deposition of CuO thin films by sputtering and for a use as positive electrode in lithium microbatteries.[22,23] This study deals with the preparation by reactive magnetron sputtering and a thorough physico-chemical characterization of copper oxide thin films. The influence of various parameters such as oxygen flow rate, substrate temperature, substrate-target distance, total pressure and target orientation (horizontal or tilted) was investigated with the aim to tailor the film properties giving the best electrochemical performances. The results provide an insight on how these sputtering parameters influence the deposition rate, the chemical composition, the structure and the morphology of these thin films. Preliminary electrochemical results highlight that CuO thin film performance is strongly related to its morphology and structure.

2. EXPERIMENTAL SECTION

2.1. Preparation of Copper Oxide Thin Films. Thin films were prepared by radio frequency magnetron sputtering in a Plassys MP 700

Received: December 4, 2013
Accepted: February 12, 2014
Published: February 12, 2014

   dx.doi.org/10.1021/am4055386 | ACS Appl. Mater. Interfaces 2014, 6, 3413−3420

apparatus from a 75 mm diameter copper target in a mixed (Ar + O_2) atmosphere. Several substrates (silicon, glass, stainless steel or carbon) were used to perform the different scheduled characterizations. Before their introduction in the deposition chamber, all substrates were cleaned by using isopropanol vapor to remove any contaminants. Inside the sputtering chamber and before deposition, the substrates were also etched by argon ions (Kurt J. Lesker). The copper target was systematically pre-sputtered during 15 min in the Ar−O_2 gaseous mixture. During the deposition, the power density applied to the target was fixed equal to 2.3 W·cm^{-2}, the total gas flow rate was kept at 50 sccm and the oxygen flow rate was varied from 2 to 6 sccm (the oxygen concentration varying from 4 to 12%). Three different total pressures were used: 0.5, 1 or 1.5 Pa. During the deposition process, the substrate holder was rotating to get homogenous thin films and the substrates were either not intentionally heated or heated at 350 °C. Besides, the copper target was either parallel to the substrate holder (horizontal) or tilted by an angle of 23°, as shown in Figure S1 (Supporting Information). The substrate-to-target distance ranged between 8 and 12 cm with the horizontal target whereas the latter was fixed to 11 cm with the tilted target.

2.2. Characterization of Thin Films. The deposition rate was determined from the deposition time and the thin films thickness measured by using a Dektak 6M profilometer.

Thin film compositions were determined by RBS at a backscattering angle of 150° using an incident beam of $^4He^+$ ions with energy of 2 MeV. For that purpose, thin films with an average thickness of 100 nm were deposited onto vitreous carbon substrates. The spectra were then analysed with the SIMNRA software.[26] Auger electron spectroscopy was carried out with a VG MICROLAB 310F to check the in-depth compositional homogeneity of the thin films.

The structural properties of the thin films were studied by X-ray diffraction using a Philips Panalytical X'Pert Pro diffractometer with Co Kα radiation (λ = 1.7889 Å). Texture analysis was performed using a Panalytical X'Pert and a Bruker D8 Discover four circles diffractometer with Cu Kα radiation. Thin films deposited onto silicon or glasses substrates were used for X-ray diffraction characterizations.

The cross-section and surface morphology of the thin films were investigated by scanning electron microscopy using a Jeol 6700-F microscope. To avoid any charging of the samples by the electron beam during observations, the films were systematically coated with a thin gold film.

The electrical conductivity of selected thin films was determined by using a four point probe technique.

To carry out the electrochemical characterization of CuO thin films, these latter were deposited onto stainless steel substrates (Ø 15 mm). These substrates were weighted individually before and after the thin film deposition to precisely determine the mass of the electrode material (typically around 400 μg). Then lithium coin cells (CR2032) were assembled in an argon-filled glovebox. A lithium foil (Chemetall, battery grade) was used as the negative electrode. The separator was a bilayer of polypropylene felt (Viledon, Freundenberg) and polypropylene microporous membrane (Celgard 2400). The electrolyte used was 1M $LiPF_6$ in a 1:1:3 volumetric mixture of ethylene carbonate (EC), propylene carbonate (PC), dimethyl carbonate (DMC), with 2 wt % of vinylene carbonate (VC). The charge/discharge cycles were performed at 25 °C at a constant current density of 6.6 μA·cm^{-2} between 0.8 and 3.5 V/Li^+/Li.

3. RESULTS AND DISCUSSION

3.1. Influence of Oxygen Flow Rate on Deposition Rate, Composition and Electronic Conductivity of Thin Films. In a first stage, the influence of the oxygen flow rate, noted $Q(O_2)$, on the deposition rate of CuO thin films was studied (Figure S2, Supporting Information). The total pressure was fixed to 0.5 Pa, the target-to-substrate distance was chosen equal to 8 cm and $Q(O_2)$ was varied between 2 and 6 sccm (the total flow rate being kept at 50 sccm). Up to $Q(O_2)$ = 5 sccm, after a slight decrease, the deposition rate remains quite stable, indicating no strong poisoning of the target. Then at $Q(O_2)$ = 6 sccm, an abrupt decrease occurs. During the sputtering process, the oxygen gas that is introduced in the chamber reacts at the target surface, while the latter is bombarded by argon ions. Hence, there is a competition between the target erosion and the target oxygenation and this decrease may indicate that the latter predominates and the target surface is getting fully oxidized. Such deposition rate evolution was also reported by Pierson et al. by sputtering a copper target with a similar reactive gas mixture.[24]

Then, the influence of the oxygen flow rate on the composition of copper oxide thin films was checked. All the diffraction patterns of thin films obtained with various oxygen flow rates are displayed in Figure 1a. Thin films of Cu_2O are

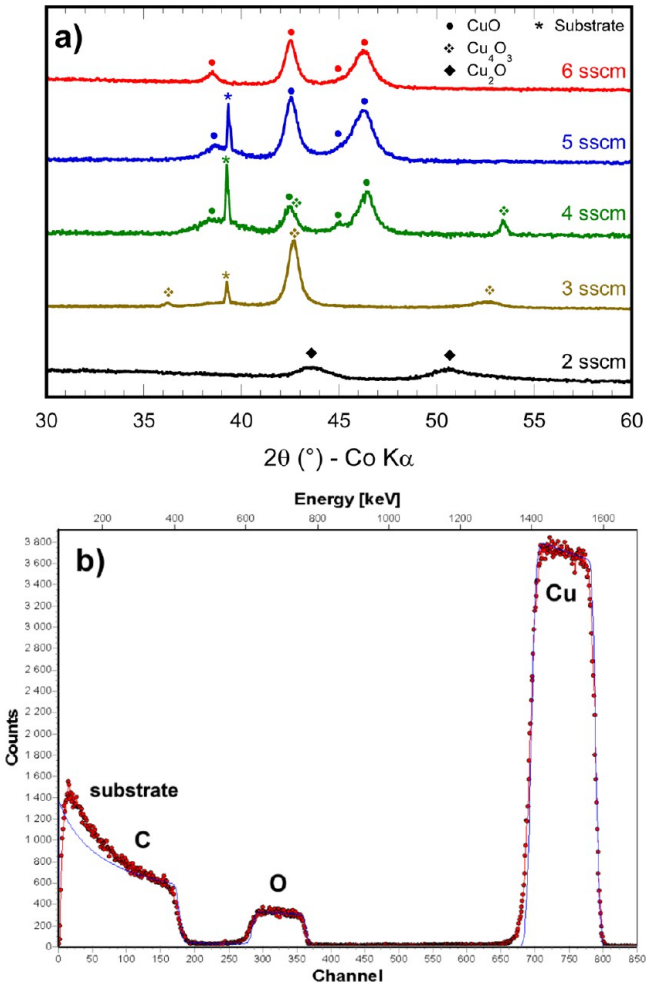

Figure 1. (a) X-ray diffraction patterns of thin films obtained with different oxygen flow rates and at a total pressure of 0.5 Pa (horizontal target, unheated substrate, target-to-substrate distance equal to 8 cm); (b) RBS spectrum of a CuO thin film deposited on a carbon substrate. Experimental data correspond to red points and the continuous line is the fitted curve using SIMNRA software.

obtained as soon as oxygen is introduced into the deposition chamber. Diffraction peaks characteristics of metallic copper are never observed. For $Q(O_2)$ = 3 sccm, peaks that could correspond to the paramelaconite phase Cu_4O_3 were obtained without any preferential orientation. The O/Cu ratio determined by RBS spectroscopy (Table 1) is close to 0.70

Table 1. Thin Film Chemical Composition Given by RBS and by XRD as a Function of the Oxygen Flow Rate

oxygen flow rate (sccm)	O/Cu ratio determined by RBS	phases identified by XRD
2	0.47 ± 0.05	Cu_2O
3	0.70 ± 0.07	Cu_4O_3
4	0.90 ± 0.09	CuO + ε Cu_4O_3
5	1.0 ± 0.1	CuO

and consistent with this phase. Cu_4O_3 is a metastable copper oxide that can be barely synthesized in a pure bulk form. However, the conditions of sputtering (more or less far from thermodynamic equilibrium) seem to enable Cu_4O_3 formation. Cu_4O_3 thin films were previously successfully prepared by sputtering from a pure copper target in a reactive gas mixture of oxygen (5 sccm) and argon (25 sccm) or by sputtering a copper oxide target in pure argon at a total pressure of 0.6 Pa.[25,27] At $Q(O_2)$ = 4 sccm, both CuO and Cu_4O_3 phases are detected, the latter being present in a minor proportion. At higher oxygen concentrations, thin films composed of a pure CuO were obtained. The O/Cu ratio was determined by RBS spectroscopy (Figure 1b and Table 1), the results being in agreement with the XRD patterns. Moreover, depth composition profiles were determined by Auger electron spectroscopy and demonstrated the compositional homogeneity over the whole thickness (Figures S4, S5 and S6, Supporting Information) .

The electrical conductivity of stoichiometric thin films prepared at $Q(O_2)$ = 5 and 6 sccm was measured under ambient atmosphere from room temperature to 100 °C. As expected for a semiconducting material, their electrical conductivity increases with temperature. Its linear evolution allows the determination of their activation energy according to an Arrhenius law. The values of conductivity and activation energy are reported in Table 2 for CuO thin films. Both values

Table 2. Effect of the Oxygen Flow Rate on the Electrical Conductivity of CuO Thin Films Deposited onto Unheated Substrates at a Total Pressure of 0.5 Pa (Horizontal Target)

oxygen flow rate (sccm)	electrical conductivity ($S \cdot cm^{-1}$)	activation energy (eV)
5	$3.9 \times 10^{-3} \pm 0.4 \times 10^{-3}$	0.25
6	$9.3 \times 10^{-3} \pm 0.1 \times 10^{-3}$	0.11

reported for the highest oxygen concentration are consistent with the ones reported for CuO thin films, the activation energy value being typical of a polaron-assisted conduction mechanism.[5,28,29] The higher value of activation energy and the lower electrical conductivity of thin films prepared at $Q(O_2)$ = 5 sccm indicates a lower number of charge carriers and/or a lower mobility of charge carriers in these thin films. Finally, the composition of the sputtered films is strongly dependent on the oxygen flow rate. Both 5 and 6 sscm oxygen flow rates allow the preparation of stoichiometric CuO, but due to the higher conductivity of the thin films obtained with the oxygen richest atmosphere, the optimized oxygen flow rate of 6 sccm (corresponding to an oxygen concentration of 12%) was chosen for further experiments in order to facilitate the first lithium electrochemical insertion.

3.2. Effect of Other Sputtering Parameters (Substrate Temperature, Total Pressure and Target-Substrate Distance) On Structure and Morphology of Thin Films Prepared with a Horizontal Target.

To investigate the effect of substrate temperature, thin films were prepared at 350 °C while other thin films were prepared without any intentional heating of the substrate holder during deposition.

Thin films deposited onto a substrate heated at 350 °C exhibit a slightly better crystallinity as shown on Figure 2. The indexation of the diffraction peaks is based on the monoclinic cell, with the space group $C\,2/c$.[30]

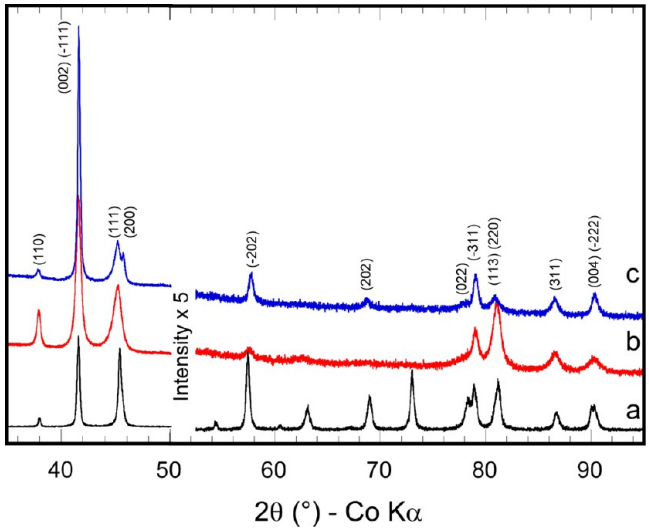

Figure 2. X-ray diffraction patterns of a commercial CuO powder (Sigma Aldrich) (a) and thin films prepared with an horizontal target, an oxygen concentration of 12%, on a substrate intentionally heated at 350 °C at a total pressure of 0.5 Pa (b) or 1 Pa (c).

In both cases, thin films all exhibit a columnar growth and a homogeneous surface (Figure S3, Supporting Information). The deposition rate and the substrate temperature are the two main parameters influencing the microstructure of the film. The change in the surface morphology of the copper oxide thin films can be understood by the Thornton zone model.[31] This model predicts three structural zones as a function of T/Tm where T is the substrate temperature and Tm is the melting temperature. As the substrate temperature does not exceed 350 °C, all thin films are grown in zone 1 where the main process is shadowing (simple geometric interactions between roughness of the growing surface and the angular directions of the arriving sputtered atoms). In this case, adatom diffusion is insufficient to overcome the effects of shadowing. Whenever a significant oblique component is present in the incident beam flux of atoms, open boundaries are induced because the high point on the growing surface receives more flux than the valleys. The zone 1 structure is typical of films grown under conditions of low adatom mobility with the incident particle energy less than 1 eV.

The influence of the total pressure was also studied on thin films prepared at 350 °C and with a target-substrate distance equal to 8 cm. As the total pressure increases from 0.5 to 1 Pa, two opposite phenomena coexist: more gas species are present in the chamber, which favors the sputtering process, but the sputtered particles undergo more collisions with the gas species concomitant with a decrease of the mean free path. The latter phenomenon is predominant when the total pressure increases from 0.5 to 1 Pa (from 32.2 ± 0.4 to 14.4 ± 0.5 $nm \cdot min^{-1}$), as the deposition rate is divided by more than a factor 2. So, when

dx.doi.org/10.1021/am4055386 | ACS Appl. Mater. Interfaces 2014, 6, 3413−3420

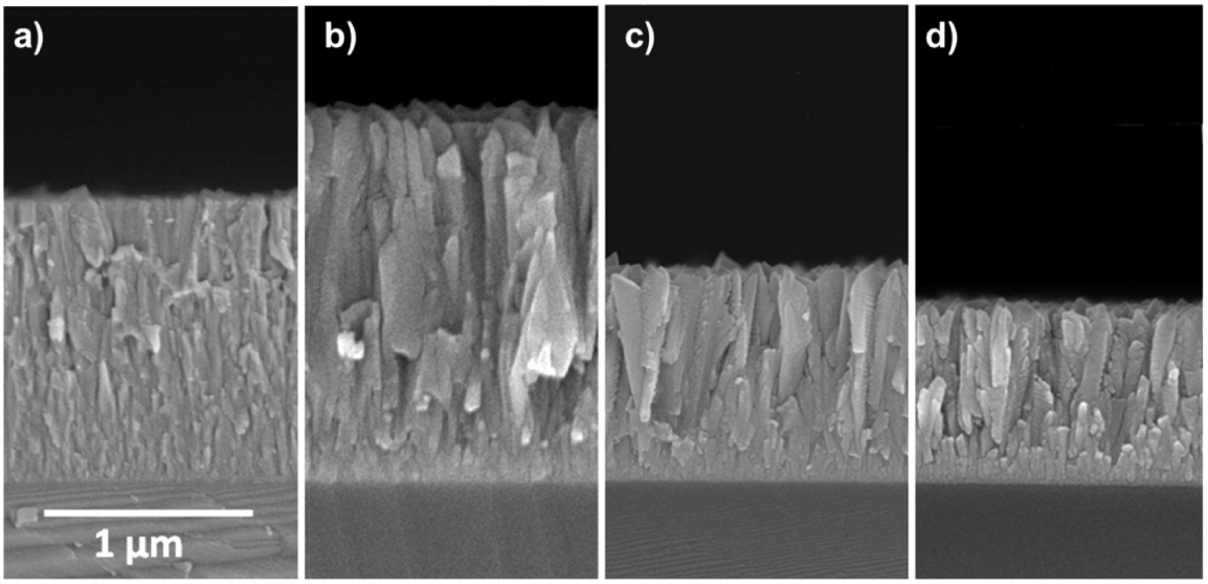

Figure 3. SEM cross sections of thin films deposited onto a silicon heated substrate (350 °C) with a target-substrate distance (dt-s) equal to 8 cm at a total pressure of (a) 0.5 Pa and (b) 1 Pa or at a total pressure of 1 Pa and (c) (dt-s) equal to 10 cm and (d) (dt-s) equal to 12 cm.

the total pressure is decreased, an increase in the energetic particle bombardment occurs, resulting in densification of the film (Figure 3a,b). The column average diameter can be estimated around 120−140 nm for thin films prepared at 1 Pa.

Consequently, the increase of the total pressure also influences the thin film structure. Obviously, there is a preferential orientation for the thin film prepared at a total pressure of 1 Pa (Figure 2). As the (002) peak cannot be easily separated from the (−111) reflection peak, as well as for the set of diffraction peaks {(004); (−222)}, it is not possible to conclude on whether this preferred orientation corresponds to (00*l*) plane or to (−hhh) plane.

The target-substrate distance was varied from 8 to 12 cm to investigate its influence for thin films deposited at 350 °C for a total pressure of 1 Pa. As expected, the deposition rate strongly decreases when the target-to-substrate distance varies from 8 to 12 cm (Table 3). Indeed, with a higher target-to-substrate

Table 3. Effect of Target-Substrate Distance on Deposition Rate of Thin Films Prepared with a Horizontal Target at a Total Pressure of 1 Pa and Deposited onto Substrates Heated to 350 °C

substrate-target distance (cm)	deposition rate (nm·min^{-1})
8	14.4 ± 0.5
10	12.7 ± 0.3
12	6.0 ± 0.6

distance, sputtered particles undergo more collisions with gas species and are more scattered before reaching the substrate. Moreover, as the sputtering is achieved approximately conically from the target surface, a lower part of sputtered particles is intercepted by the substrate at higher target-to-substrate distances. As previously mentioned, a columnar growth was observed for each of these thin films (Figures 3). However, when a longer target-substrate distance is used, the thin film morphology evolves toward more faceted columns having a pyramidal head. Whatever the target-to-substrate distances, these thin films are crystalline (Figure 4). With a higher target-to-substrate distance, an increase of the strong double peak

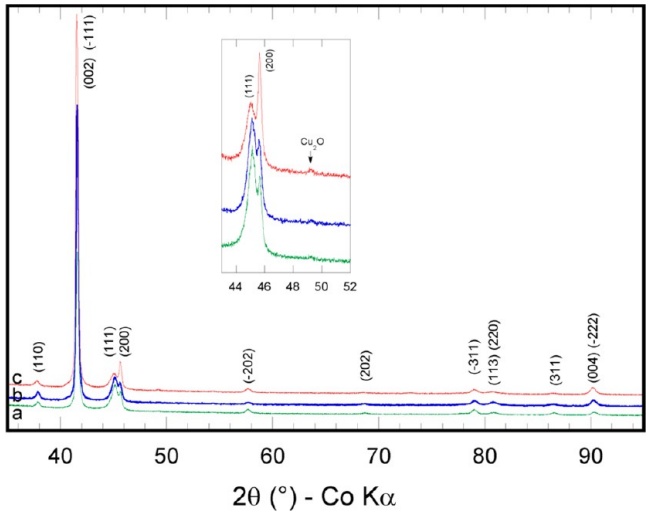

Figure 4. X-ray diffraction patterns of thin films deposited at a total pressure of 1 Pa onto heated substrates (350 °C) during deposition and a target-substrate distance (horizontal target) of (a) 8 cm, (b) 10 cm and (c) 12 cm.

{(002); (−111)} intensity, characteristic of a preferred orientation, is noticed, as well as the intensity of the (200) peak. Moreover, some peaks are slightly shifted to lower angles. As this shift depends on the reflection considered, it might be due to the presence of microstrains in theses thin films or more likely to the presence of a slight deviation from the CuO stoichiometry.[32,33] With an increasing target-substrate distance, sputtered particles collide with the substrate with a lower energy, which favors thin films having preferred orientations and a columnar morphology. For the highest target-substrate distance (12 cm), a little diffraction peak attributed to plane (200) of Cu_2O is also present. A slight oxygen deficiency is observed by Auger spectroscopy near the outer surface of the film. This suggests that this minor Cu_2O phase is mainly located at the surface of the film.

3.3. Effect of Other Sputtering Parameters on Structure and Morphology of Thin Films Prepared

dx.doi.org/10.1021/am4055386 | ACS Appl. Mater. Interfaces 2014, 6, 3413−3420

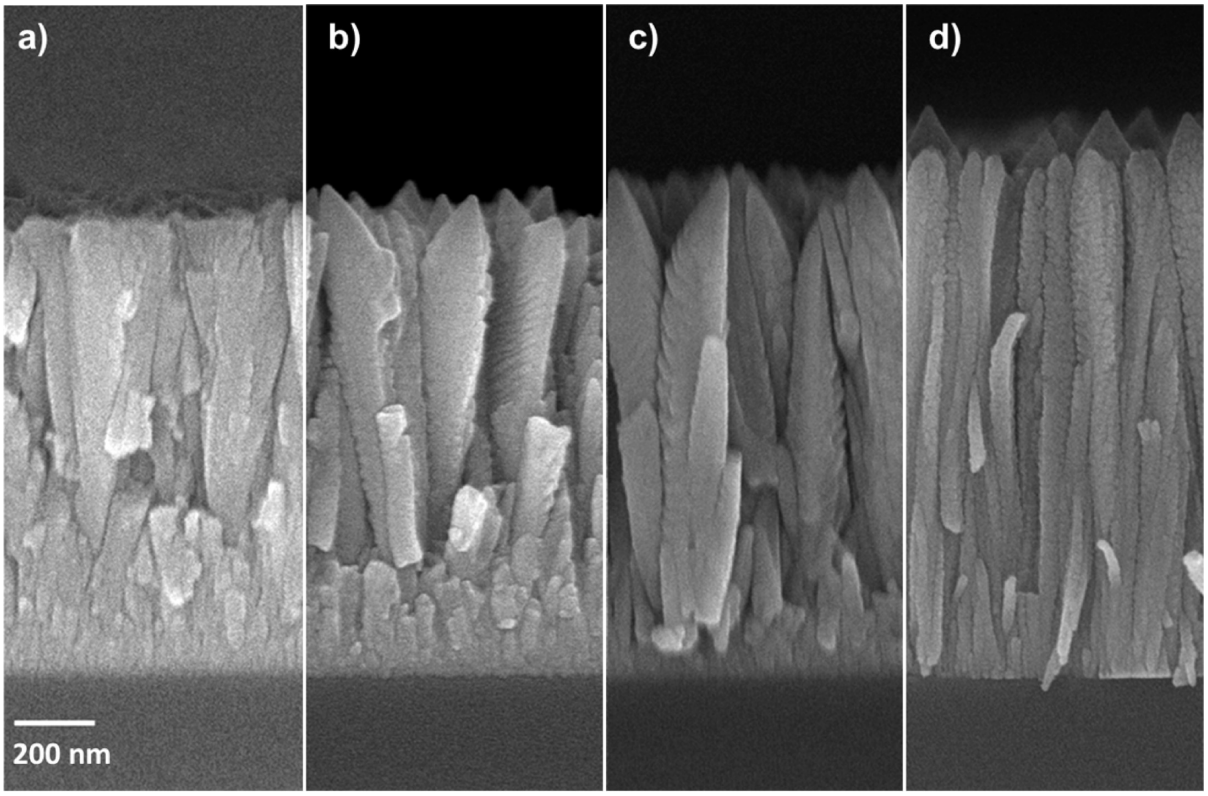

Figure 5. SEM cross sections of thin films obtained by using a tilted target and deposited onto heated substrates (350 °C) at a total pressure of (a) 0.5 Pa, (b) 1 Pa and (c) 1.5 Pa or (d) on an unheated substrate at 1.5 Pa.

with a Tilted Target. In the case of a horizontal configuration, we demonstrated that the increase of total pressure or of the target-substrate distance induces a lower deposition rate and favors thin films having a strong preferred orientation and a columnar morphology, less and less dense. Other thin films were prepared by using a tilted target to get an even less dense morphology. A porous morphology is convenient in liquid electrolyte to allow better lithium diffusion and to accommodate volumetric expansion (close to 80% for the insertion of two lithium ions). The physico-chemical properties of these thin films were investigated as a function of the total pressure and of the substrate temperature.

The influence of the total pressure was studied for thin films deposited on a heated substrate (350 °C) at a total pressure of 0.5, 1 or 1.5 Pa. As observed with a horizontal target, an increase of the total pressure also induces here a decrease of the deposition rate. The deposition rate obtained at 1 Pa is 5.2 ± 0.7 nm·min^{-1}, which is similar to the deposition rate with a horizontal target fixed at a distance of 12 cm from the substrate. The SEM cross-section images of these thin films deposited onto a silicon substrate are shown in Figure 5. It has to be noticed that these thin films exhibit a columnar growth perpendicular to the substrate and do not show a tilted growth, as it would have been expected, which is probably due to the fact that the substrate holder is rotating during deposition. A less dense morphology, without a noticeable change of the mean average column diameter, is observed for thin films prepared at higher total pressures. Moreover, each column consists of stacking platelets of about 10−20 nm in height, particularly for thin films prepared at 1 and 1.5 Pa, illustrating the adatom surface diffusion that occurs during thin films growth.

As seen previously, the increase of total pressure means also that sputtered particles impact the substrate with a lower energy, which favors preferred orientations (Figure 6). It can

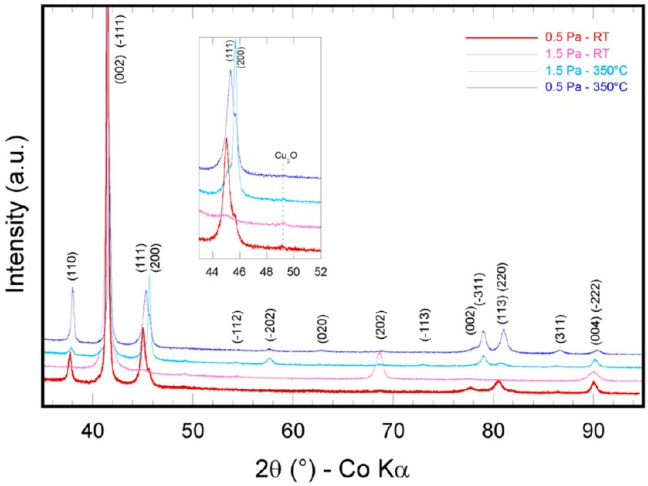

Figure 6. X-ray diffraction patterns of thin films obtained by using a tilted target and deposited at a total pressure of either 1.5 or 0.5 Pa, onto a substrate either unheated or heated at 350 °C during deposition.

also be observed for thin films prepared at 1.5 Pa, a strong intensity for plane (200). Moreover, an extra diffraction peak, characteristic of the Cu_2O phase, with a very low intensity is observed at 49.2° for thin films prepared at 1 and 1.5 Pa.

Thin films prepared by using a tilted target were also deposited onto an unheated substrate. A total pressure of 0.5, 1

dx.doi.org/10.1021/am4055386 | ACS Appl. Mater. Interfaces 2014, 6, 3413−3420

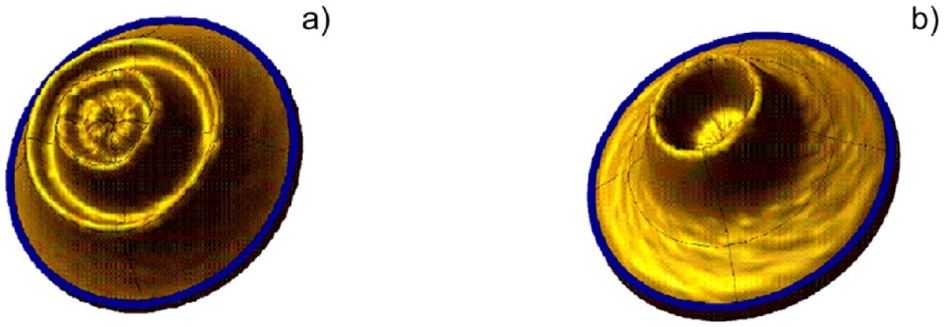

Figure 7. Pole figures of a thin film deposited at 1.5 Pa onto an unheated substrate for (a) 110 peak and (b) 020 peak.

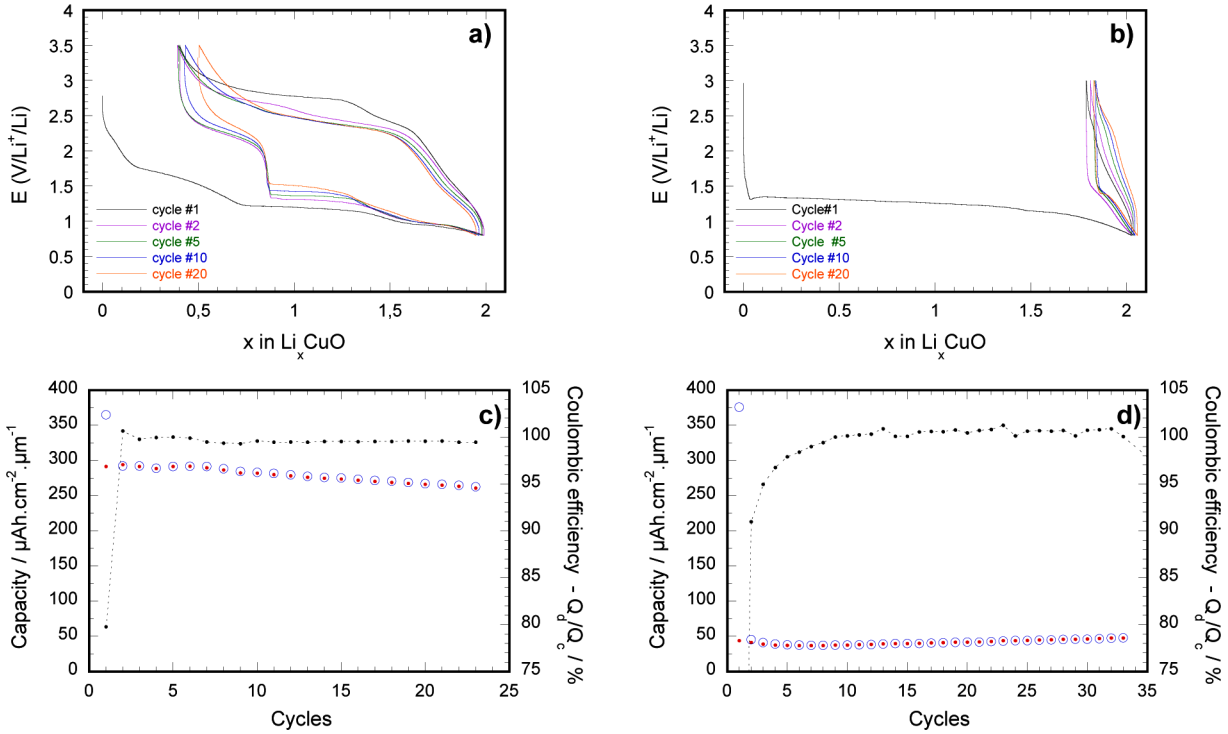

Figure 8. Galvanostatic charge/discharge curves of (a) a thin film (570 nm thick) prepared with a tilted target onto an unheated substrate at a total pressure of 1.5 Pa (sample A) and (b) a thin film (680 nm thick) prepared at 0.5 Pa but with a horizontal target and a substrate heated at 350 °C (sample B). Evolution of the corresponding electrode capacities upon cycling for films prepared on (c) unheated or (d) heated substrates.

and 1.5 Pa was applied and the same tendency previously described was observed, namely a decrease of deposition rate, a columnar morphology getting more porous and a more preferred orientation in thin films as the total pressure increases. The morphology of thin films prepared at a total pressure of 1.5 Pa as a function of temperature during deposition (substrates heated at 350 °C or unheated) is displayed in Figure 5c,d, respectively. The increase in column size for thin film deposited at 350 °C with respect to the film deposited at room temperature matches well with the theoretical predictions of the Thornton model. Thin films deposited on unheated substrate (Figure 5d) exhibit rod-shaped columns having an average diameter less than 100 nm and a less dense morphology as their thickness is slightly increased compared to those prepared on heated substrates (for same deposition conditions). The crystallinity of these thin films is lower and less diffraction peaks are visible (Figure 6). The presence of a very low intensity diffraction peak attributed to Cu_2O can be noticed. The presence of a small amount of this phase is suggested again near the surface both by the results of Auger depth profiling analyses and by XPS measurements which show the presence of a small amount of Cu^+.[32] A strong {(002); (−111)} preferred orientation is observed for the CuO phase. Furthermore, the strong intensity of its (202) diffraction peak observed for thin films prepared with an unheated substrate clearly suggests that the substrate temperature also influences the texture of these thin films. A complete study of crystallographic textures of two films deposited at a total pressure of 1.5 Pa on an unheated substrate and a substrate heated at 350 °C was carried out. For both films, the measured pole figures exhibit rotational symmetry evidencing fiber textures, which is a usual result for in plane sputtering deposition (Figure 7). Taking into account the reinforcements of diffracted intensity as a function of tilt angle for various crystallographic planes, one succeeded to determine the main fiber axis in each case: it is close to the (−61, 100, 78) plane normal for the unheated substrate and close to the (−100, 4, 32) normal for the 350 °C heated substrate. Because of the low symmetry monoclinic structure of CuO, it is not surprising to obtain such complex growth directions. One possible

dx.doi.org/10.1021/am4055386 | ACS Appl. Mater. Interfaces 2014, 6, 3413−3420

explanation for this could be a stresses-driven mechanism linked to the elastic anisotropy of such crystals. It is worth noting that theses textures are not sharp, and a disorientation of about 10° from the main direction is observed in both films. In addition, some intensity reinforcements cannot be explained by the main fiber axis revealing some others minor fiber components. These thin films prepared with a tilted target were found to have a slightly lower density than their counterparts prepared with a horizontal target with, respectively, a minimum value of about 76% and a maximum value of 82% of the CuO theoretical density (6.31 $g \cdot cm^{-3}$).

3.4. Electrochemical Characterization in Li Coin Cells. Although the theoretical capacity corresponding to the insertion of 2 Li/CuO is always reached at the end of the first reduction (0.8 $V/Li^+/Li$) for all CuO films (prepared with a horizontal or a tilted target), the reversibility of the conversion reaction is greatly enhanced for the films obtained on an unheated substrate with a tilted target (Sample A, Figure 8a,c). Indeed, a reversible capacity as high as 1.6 Li/CuO was obtained for this sample. The reversibility of the conversion reaction is then maintained at this level at least for 20 cycles. The initial discharge capacity of 375 $\mu Ah \cdot cm^{-2} \cdot \mu m^{-1}$ corresponds to about 90% of the theoretical volumetric value (425 $\mu Ah \cdot cm^{-2} \cdot \mu m^{-1}$). The practical reversible capacity of the last cycles is then close to 300 $\mu Ah \cdot cm^{-2} \cdot \mu m^{-1}$, which corresponds to 1.6 Li/CuO or 540 $mAh \cdot g^{-1}$. On the contrary, the material deposited at 350 °C with a horizontal target (Sample B, Figure 8b,d) exhibits the lowest reversible capacity, corresponding to the deinsertion of only 0.2 Li/CuO during the first charge and subsequent cycles.

Comprehensive studies aiming to determine the mechanisms involved in the transformation of the CuO thin film electrode during lithium insertion/desinsertion were carried out on the best sample (unheated substrate, 1 Pa, 12% O_2, tilted target) using XPS and AFM techniques and are reported in previous papers.[34,35] It was found that the electrolyte starts to react with the surface of the CuO electrode from 1.4 $V/Li^+/Li$ onwards during the first reduction, forming a solid electrolyte interphase (SEI) layer. As for the bulk electrode material, a three-step reduction process, involving a peroxide intermediate, was proposed:

$$CuO + 1/2\ Li \rightarrow 1/2\ Cu_2O + 1/4\ Li_2O_2 \quad (\sim 1.7\ V/Li^+/Li) \qquad \text{(Step I)}$$

$$1/2\ Cu_2O + 1/4\ Li_2O_2 + Li \rightarrow Cu + 1/4\ Li_2O_2 + 1/2\ Li_2O\ (\sim 1.2\ V/Li^+/Li) \qquad \text{(Step II)}$$

$$Cu + 1/4\ Li_2O_2 + 1/2\ Li_2O + 1/2\ Li \rightarrow Cu + Li_2O\ (\sim 0.9\ V/Li^+/Li) \qquad \text{(Step III)}$$

During the subsequent delithiation, only the two last steps located, respectively, oxidation around 2.4 $V/Li^+/Li$ (III) and 2.8 $V/Li^+/Li$ (II) were found to be reversible. Depth-profiling XPS analyses showed that the reduction processes spread from the thin film surface to the current collector, but that the oxidation starts at the surface of the current collector. This clearly highlights that the low electronic conductivity of the [Cu, Li_2O] matrix is the limiting factor for the electrochemical reaction. Moreover, it was evidenced that the volume changes between the lithiated and delithiated states lead to the formation of cracks in the copper oxide film and to matter extrusion.

From these previous studies, the limited Li deinsertion in sample B could be explained by either (i) a rapid loss of electronic contact between the [Cu, Li_2O] matrix and the current collector at the beginning of the oxidation, as the latter begins at this interface and involves a shrinkage of the material or (ii) the conversion reaction itself, which induces the formation of a less percolated Cu conductive array inside the insulating Li_2O matrix, preventing the reversibility of the reaction. The influence of the metallic nanoarray distribution inside the final product of the conversion reaction on the reversibility of the reaction was clearly demonstrated for example in FeF_2 and CuF_2 compounds.[36]

4. CONCLUSION

Copper oxide thin films were prepared by reactive sputtering of a pure copper target in a mixture of argon and oxygen optimized at 0.5 Pa with an oxygen concentration of 12%. Through increases to the total pressure or the target-substrate distance, thin films showed a columnar growth and preferred orientations more and more pronounced. At a high target-substrate distance, despite an oxygen flow rate of 12 sccm, Cu_2O as a minor phase is detected, Auger depth-profiling results suggest it is mainly located near the film surface. Thin films having a better crystallinity were obtained by heating the substrate at 350 °C during deposition. Moreover, the use of a tilted target, the substrate holder being rotated during deposition, enables to achieve thin films strongly textured and having different morphologies, depending on the substrate temperature and on the total pressure. These films exhibit complex fiber textures. The main fiber axes are normal to high Miller indices planes and vary with the substrate temperature. The best electrochemical performances were obtained for thin films prepared with a tilted target and deposited at a total pressure of 1.5 Pa onto unheated substrates. The reversible volumetric capacity is close to 300 $\mu Ah \cdot cm^{-2} \cdot \mu m^{-1}$, which exceeds, by far, the volumetric capacity of insertion materials currently used as positive electrode in lithium microbattery, such as $LiCoO_2$ (64 $\mu Ah \cdot cm^{-2} \cdot \mu m^{-1}$) or TiO_yS_z (90 $\mu Ah \cdot cm^{-2} \cdot \mu m^{-1}$).[37,38] Further experiments will consist in preparing all-solid-state cells with a solid electrolyte and comparing their performances with those obtained in coin cells with a liquid electrolyte.

■ ASSOCIATED CONTENT

Supporting Information

Illustration of the target positioning in horizontal or tilted configurations, plot of the deposition rate versus the oxygen concentration, top-view of some film surfaces and Auger depth-profiling analyses of CuO films prepared in various conditions. This material is available free of charge via the Internet at http://pubs.acs.org.

■ AUTHOR INFORMATION

Corresponding Authors

*B. Pecquenard. E-mail: pecquen@icmcb-bordeaux.cnrs.fr.
*F. Le Cras. E-mail: frederic.lecras@cea.fr.

Notes

The authors declare no competing financial interest.

■ ACKNOWLEDGMENTS

The authors thank L. Teule-Gay for his help in sputtering experiments and Stéphanie Sorieul from AIFIRA for her help in acquiring RBS spectra.

■ REFERENCES

(1) Sung, S.-Y.; Kim, S.-Y.; Jo, K.-M.; Lee, J.-H.; Kim, J.-J.; Kim, S.-G.; Chai, K.-H.; Pearton, S. J.; Norton, D. P.; Heo, Y.-W. Fabrication of p-channel thin-film transistors using CuO active layers deposited at low temperature. *Appl. Phys. Lett.* **2010**, *97*, 222109.

(2) Kim, S.; Hong, K.; Kim, K.; Lee, I.; Kim, K.-B.; Lee, D.Y.; Kim, T.-Y.; Lee, J.-L. Hole injection layer of thermally evaporated copper oxide for top emitting organic light emitting diodes. *J. Electrochem. Soc.* **2010**, *157*, J347−J350.

(3) Yoon, K. H.; Choi, W. J.; Kang, D. H. Photoelectrochemical properties of copper oxide thin films coated on an n-Si substrate. *Thin Solid Films* **2000**, *372*, 250−256.

(4) Ogwu, A.A.; Bouquerel, E.; Ademosu, O.; Moh, S.; Crossan, E.; Placido, F. An investigation of the surface energy and optical transmittance of copper oxide thin films prepared by reactive magnetron sputtering. *Acta Mater.* **2005**, *53*, 5151−5159.

(5) Paretta, A.; Jayaraj, M. K.; Di Nocera, A.; Loreti, S.; Quercia, L .; Agati, A. Electrical and optical properties of copper oxide films prepared by reactive RF magnetron sputtering. *Phys. Status Solidi A* **1996**, *155*, 399−404.

(6) Reitz, J. B.; Solomon, E. I. Propylene oxidation on copper oxide surfaces: Electronic and geometric contributions to reactivity and selectivity. *J. Am. Chem. Soc.* **1998**, *120*, 11467−11478.

(7) Li, D.; Hu, J.; Wu, R.; Lu, J. G. Conductometric chemical sensor based on individual CuO nanowires. *Nanotechnology* **2010**, *21*, 485502.

(8) Bates, R.; Jumel, Y. In *Lithium Batteries*; Gabano, J.-P., Ed.; Academic Press: London, 1983; pp 73−94.

(9) Poizot, P.; Laruelle, S.; Grugeon, S.; Dupont, L.; Tarascon, J.-M. Nano-sized transition-metal oxides as negative-electrode materials for lithium-ion batteries. *Nature* **2000**, *407*, 496−499.

(10) Tarascon, J.-M.; Grugeon, S.; Morcrette, M.; Laruelle, S.; Rozier, P.; Poizot, P. New concepts for the search of better electrode materials for rechargeable lithium batteries. *C. R. Chim.* **2005**, *8*, 9−15.

(11) Tarascon, J.-M.; Armand, M. Issues and challenges facing rechargeable lithium batteries. *Nature* **2001**, *414*, 359−367.

(12) Grugeon, S.; Laruelle, S.; Herrera-Urbina, R.; Dupont, L.; Poizot, P.; Tarascon, J. -M. Particle size effects on the electrochemical performance of copper oxides toward lithium. *J. Electrochem. Soc.* **2001**, *148*, A285−A292.

(13) Xiang, J. Y.; Tu, J. P.; Zhang, L.; Zhou, Y.; Wang, X. L.; Shi, S. J. Self-assembled synthesis of hierarchical nanostructured CuO with various morphologies and their application as anodes for lithium ion batteries. *J. Power Sources* **2010**, *195*, 313−319.

(14) Park, J. C.; Kim, J.; Kwon, H.; Song, H. Gram-scale synthesis of Cu_2O nanocubes and subsequent oxidation to CuO hollow nanostructures for lithium-ion battery anode materials. *Adv. Mater.* **2009**, *21*, 803−807.

(15) Dar, M. A.; Nam, S. H.; Kim, Y. S.; Kim, W. B. Synthesis, characterization, and electrochemical properties of self-assembled leaf-like CuO nanostructures. *J. Solid State Electrochem.* **2010**, *14*, 1719−1726.

(16) Gao, X. P.; Bao, J. L.; Pan, G. L.; Zhu, H. Y.; Huang, P. X.; Wu, F.; Song, D. Y. Preparation and electrochemical performance of polycrystalline and single crystalline CuO nanorods as anode materials for Li ion battery. *J. Phys. Chem. B* **2004**, *108*, 5547−5551.

(17) Chen, L. B.; Lu, N.; Xu, C. M.; Yu, H. C.; Wang, T. H. Electrochemical performance of polycrystalline CuO nanowires as anode material for Li ion batteries. *Electrochim. Acta* **2009**, *54*, 4198−4201.

(18) Pan, Q.; Jin, H.; Wang, H.; Yin, G. Flower-like CuO film-electrode for lithium ion batteries and the effect of surface morphology on electrochemical performance. *Electrochim. Acta* **2007**, *53*, 951−956.

(19) Morales, J.; Sánchez, L.; Martín, F.; Ramos-Barrado, J. R.; Sánchez, M. Use of low-temperature nanostructured CuO thin films deposited by spray-pyrolysis in lithium cells. *Thin Solid Films* **2005**, *474*, 133−140.

(20) Xiang, J. Y.; Tu, J. P.; Yuan, Y. F.; Wang, X. L.; Huang, X. H.; Zeng, Z. Y. Electrochemical investigation on nanoflower-like CuO/Ni composite film as anode for lithium ion batteries. *Electrochim. Acta* **2009**, *54*, 1160−1165.

(21) Barrecca, D.; Carraro, G.; Gasparotto, A.; Maccato, C.; Cruz-Yusta, M.; Gomez-Camer, J. L.; Morales, J.; Sada, C.; Sanchez, L. On the preformances of CuxO-TiO2 (x=1,2) nanomaterials as innovative anodes for thin film lithium batteries. *ACS Appl. Mater. Interfaces* **2012**, *4*, 3610−3619.

(22) Feng, J. K.; Xia, H.; Lai, M. O.; Lu, L. Electrochemical performance of CuO nanocrystal film fabricated by room temperature sputtering. *Mater. Res. Bull.* **2011**, *46*, 424−427.

(23) Souza, E. A.; Landers, R.; Cardoso, L. P.; Cruz, T. G. S.; Tabacniks, M. H.; Gorenstein, A. Evaluation of copper oxide thin films as electrodes for microbatteries. *J. Power Sources* **2006**, *155*, 358−363.

(24) Pierson, J. F.; Wiederkehr, D.; Billard, A. Reactive magnetron sputtering of copper, silver, and gold. *Thin Solid Films* **2005**, *478*, 196−205.

(25) Pierson, J. F.; Thobor-Keck, A.; Billard, A. Cuprite, para-melaconite and tenorite films deposited by reactive magnetron sputtering. *Appl. Surf. Sci.* **2003**, *210*, 359−367.

(26) Mayer, M. *SIMNRA user's guide*, Tech. Rep. IPP 9/113; Max Planck Institut für Plasmaphysik: Garching, Germany, 1997.

(27) Blobaum, K. J.; Van Heerden, D.; Wagner, A. J.; Fairbrother, D. H.; Weihs, T. P. Sputter-deposition and characterization of para-melaconite. *J. Mater. Res.* **2003**, *18*, 1535−1542.

(28) Figueiredo, V.; Elangovan, E.; Gonçalves, G.; Franco, N.; Alves, E.; Park, S.; Martins, R.; Fortunato, E. Electrical, structural and optical characterization of copper oxide thin films as a function of post annealing temperature. *Phys. Status Solidi A* **2009**, *206*, 2143−2148.

(29) Roy, B. N.; Wright, T. Electrical conductivity in polycrystalline copper oxide thin films. *Cryst. Res. Technol.* **1996**, *3*, 1039−1044.

(30) Åsbrink, S.; Norrby, L. J. A refinement of the crystal structure of copper(II) oxide with a discussion of some exceptional e.s.d.'s. *Acta Crystallogr.* **1970**, *B26*, 8−15.

(31) Thornton, J. A. High rate thick film growth. *Ann. Rev. Mater. Sci.* **1977**, *7*, 239−260.

(32) Langford, J. I.; Louër, D. High-resolution powder diffraction studies of copper(II) oxide. *J. Appl. Crystallogr.* **1991**, *24*, 149−155.

(33) Carel, C.; Mouallem-Bahout, M.; Gaudé, J. Re-examination of the non-stoichiometry and defect structure of copper(II) oxide or tenorite, $Cu_{1\pm z}O$ or $CuO_{1\pm\varepsilon}$: A short review. *Solid State Ionics* **1999**, *117*, 47−55.

(34) Martin, L.; Martinez, H.; Poinot, D.; Pecquenard, B.; Le Cras, F. Comprehensive X-ray photoelectron spectroscopy study of the conversion reaction mechanism of CuO in lithiated thin film electrodes. *J. Phys. Chem. C* **2013**, *117*, 4421−4430.

(35) Martin, L.; Martinez, H.; Poinot, D.; Pecquenard, B.; Le Cras, F. Direct observation of important morphology and composition changes at the surface of the CuO conversion material in lithium batteries. *J. Power Sources* **2014**, *248*, 861−873.

(36) Wang, F.; Robert, R.; Chernova, N.A.; Pereira, N.; Omenya, F.; Badway, F.; Hua, X.; Ruotolo, M.; Zhang, R.; Wu, L.; Volkov, V.; Su, D.; Key, B.; Stanley Whittingham, M.; Grey, C.P.; Amatucci, G.G.; Zhu, Y.; Graetz, J. Conversion reaction mechanisms in lithium ion batteries: Study of the binary metal fluoride electrodes. *J. Am. Chem. Soc.* **2011**, *133*, 18828−18836.

(37) Wang, B.; Bates, J. B.; Hart, F. X.; Sales, B. C.; Zuhr, R. A.; Robertson, J. D. Characterization of thin film rechargeable lithium batteries with lithium cobalt oxide cathodes. *J. Electrochem. Soc.* **1996**, *143*, 3203−3213.

(38) Fleutot, B.; Pecquenard, B.; Le Cras, F.; Delis, B.; Martinez, H.; Dupont, L.; Guy-Bouyssou, D. Characterization of all-solid-state Li/LiPONB/TiOS microbatteries produced at the pilot scale. *J. Power Sources* **2011**, *196*, 10289−10296.